Journal of King Saud University – Science 33 (2021) 101317

Contents lists available at ScienceDirect

Journal of King Saud University – Science

journal homepage: www.sciencedirect.com

Original article

Bifunctional electro-catalytic performances of $NiMoO_4$-NRs@RGO nanocomposites for oxygen evolution and oxygen reduction reactions

Jahangeer Ahmed [a,*], Manawwer Alam [a], M.A. Majeed Khan [b], Saad M. Alshehri [a]

[a] Department of Chemistry, College of Science, King Saud University, Riyadh 11451, Saudi Arabia
[b] King Abdullah Institute for Nanotechnology, King Saud University, Riyadh 11451, Saudi Arabia

ARTICLE INFO

Article history:
Received 13 November 2020
Revised 3 December 2020
Accepted 17 December 2020
Available online 26 December 2020

Keywords:
$NiMoO_4$-NRs@RGO
Nanocomposite
Electro-catalysts
OER
ORR

ABSTRACT

In present study, we report hydrothermal synthesis of reduced graphene oxide (RGO) supported $NiMoO_4$-nanorods (NRs) nanocomposites ($NiMoO_4$-NRs@RGO nanocomposites) for electro-catalysis of water to oxygen evolution and reduction reactions (OER/ORR). The prepared nanocomposites were characterized by x-ray diffraction (XRD), Raman, Fourier transform infrared (FTIR), high resolution transmission electron microscopy (HRTEM), field emission scanning electron microscopy (FESEM), energy dispersive and x-ray photoelectron spectroscopy (XPS) techniques. The electrochemical performances of $NiMoO_4$-NRs@RGO nanocomposites were examined in 0.5 M KOH (alkaline electrolyte) using cyclic voltammetry (CV), linear sweep voltammetry (LSV), Tafel and chronoamperometry (CA) electrochemical techniques at room temperature. The onset over-potentials of $NiMoO_4$-NRs@RGO nanocomposite for ORR and OER were found to be of ~75 and ~185 mV, respectively, while the Tafel slopes for OER and ORR were observed to be ~54 and ~245 mV/dec respectively. The involved electrons (i.e. $4e^-$) in redox reactions were calculated using rotating disc electrode experiments. Based on admirable electro-catalytic performance of $NiMoO_4$-NRs@RGO nanocomposites with low energy loss, suggesting it as cost effective and efficient OER/ORR electro-catalysts compared to noble metal electro-catalysts.

1. Introduction

The development of the clean and sustainable energy resources is the current challenge of the researchers to overcome energy crisis globally. Splitting of water by electrochemical process to produce clean and sustainable energy is one of the alternative approaches. Electrochemical splitting of water could consist of three reactions i.e. oxygen evolution reactions (OER, anodic region), oxygen reduction reactions (ORR, cathodic region) and hydrogen evolution reactions (HER, cathodic region). In the last one decade, noble metal (e.g. Ir, Ru, Pt) based nanostructured materials were used frequently as active and highly efficient electro-catalysts for water splitting reactions (Ahmed and Mao, 2016; Fang et al., 2019; Reier et al., 2012). High cost and non-commercial benefits could be main disadvantages of these electro-catalysts. To explore bifunctional/trifunctional electro-catalysts with low cost and high efficiency are highly desirable in order to develop the clean and sustainable energy resources and to control the energy crisis worldwide. Therefore, present work is focused on bifunctional electro-catalytic activities of low cost electrode materials in alkaline medium. In the recent years, nickel based molybdate materials have been widely used as electro-catalysts in water splitting for HER and OER at cathode and anode respectively (Ahmed et al., 2019b; Geng et al., 2019; Kasturi et al., 2020; Lu et al., 2020; Wang et al., 2018; Zhang et al., 2019, 2018). The water oxidation reaction suffers from slow reaction kinetics in electron-transfer process ($4e^-$) due to high energy loss (Shaner et al., 2016). To overcome these issues and to enhance the efficiency of the electro-catalysts in energy conversion, this is necessary to develop highly efficient electro-catalysts by lowering the activation energy of water oxidation reactions. Recently, carbon-based nickel molybdate nanocomposites are reported as efficient electro-catalysts to support the enhancement in the electrolysis of water because of high electrical conductivity, chemical stability and surface area (An et al., 2020). Hydrothermally synthesized

* Corresponding author.
E-mail addresses: jahmed@ksu.edu.sa (J. Ahmed), mmkhan@ksu.edu.sa (M.A. Majeed Khan), alshehri@ksu.edu.sa (S.M. Alshehri).
Peer review under responsibility of King Saud University.

Production and hosting by Elsevier

https://doi.org/10.1016/j.jksus.2020.101317
1018-3647/

$CoP_3/NiMoO_4$ hierarchical hetero-structured materials showed efficient electro-catalytic activity in water splitting with the over-potential of 347 mV to OER using 1.0 M KOH (Wang et al., 2019). $NiMoO_4$/rGO (Jinlong et al., 2017), $NiMoO_4$/C (Jiang et al., 2019; Tong et al., 2019) and $NiMoO_4$/N-doped graphene (Feng et al., 2020) nanocomposites are recently reported as high performance energy storage materials. Moreover, $NiMoO_4$ nanostructured materials have also shown importance in variety of applications including supercapacitors (Abbas et al., 2020; Anil Kumar et al., 2020; Cai et al., 2014; Moosavifard et al., 2015), sensing (Karami and Taher, 2019), photo-catalysis (Ray et al., 2018), nitro-phenol reduction (Oudghiri-Hassani and Al Wadaani, 2018) and electro-oxidation of urea (Yang et al., 2019). Previously, we have designed metal tungstate (Ahmed et al., 2018; Alshehri et al., 2018; AlShehri et al., 2017) and metal molybdate (Ahmed et al., 2019a, 2019b) nanostructured materials for multifunctional catalytic activities including energy conversion and storage. Herein, we report the hydrothermal synthesis of $NiMoO_4$-NRs@RGO nanocomposites as efficient electro-catalysts in water splitting for OER and ORR. The synthesized $NiMoO_4$-NRs@RGO nanocomposites were characterized in details using various analytical techniques including XRD, Raman, FTIR, FESEM, HRTEM, and XPS. The electrochemical performances of $NiMoO_4$-NRs@RGO nanocomposites were also investigated in details for OER/ORR activities in alkaline medium.

2. Experimental

The following reagents, as received chemicals, have been used in the preparation of $NiMoO_4$-NRs@RGO nanocomposites: Ni $(NO_3)_2{\cdot}6H_2O$ (Sigma Aldrich, 99.90%), $Na_2MoO_4{\cdot}2H_2O$ (Merck, 99.50%), $NaNO_3$ (Alfa Aesar, 99.00%), KNO_3 (Alfa Aesar, 99.00%), ethylene glycol (Sigma Aldrich) and reduced graphene oxide (RGO, Sigma Aldrich). $NiMoO_4$-NRs were produced using the molten salts method as also reported earlier (Ahmed et al., 2019b). 100 mg $NiMoO_4$-NRs and 10 mg RGO were mixed together with 2 ml ethylene glycol and 20 ml de-ionized water followed by the sonication for 15 min to make the suspension. The pH of the suspension was maintained at ~8.5 by the addition of an appropriate amount of potassium hydroxide. The prepared suspension was transported to the hydrothermal reactor and heated at 140 °C for 24 h. The dark grey colored product was obtained, followed washing by de-ionized water for several times. The resulting powder samples were then dried at 65 °C for 5 h.

The synthesized $NiMoO_4$-NRs@RGO nanocomposites were initially characterized using XRD (Bruker D-8 Advanced diffractometer), FESM (JEOL-JSM-7600F) and HRTEM (JEOL-JSM-2100F) for phase identification and surface morphology. Energy dispersive studies (EDS) of $NiMoO_4$-NRs@RGO nanocomposites were carried out for elemental analysis. FTIR (Bruker TENSOR-27) and Raman spectroscopic (Renishaw instrument) studies were used to investigate the functional groups of the materials. BET (Brunauer–Emmett–Teller) surface area of $NiMoO_4$-NRs@RGO nanocomposites were analyzed using physi-sorption instrument (Micromeritics ASAP-2020) by nitrogen adsorption–desorption isotherm. Ultra-high vacuum XPS (Kratos Axis-Ultra X-ray photoelectron spectrometer) was also used to investigate the oxidation states of the elements present in $NiMoO_4$-NRs@RGO nanocomposites.

Electro-catalytic performances of the $NiMoO_4$-NRs@RGO nanocomposites for OER/ORR activities were investigated on potentiostat–galvanostat electrochemical workstation (CHI 660E) using 0.5 M KOH electrolyte. The working electrode was prepared by preparing the slurry containing of 2.5 mg $NiMoO_4$-NRs@RGO nanocomposites as electro-catalysts, 0.50 ml isopropanol and 0.10 ml Nafion. One drop of prepared slurry has been placed on to the glassy carbon (GC, 0.07 cm^2) which is act as working electrode. The prepared working electrodes were dried at 60 °C. The loaded amount of $NiMoO_4$-NRs@RGO catalysts was maintained of ~0.22 mg/cm^2. Pt-wire and Ag/AgCl electrodes work as counter and reference electrodes, respectively. Electro-catalytic measurements including CV, LSV, Tafel and CA were carried out for OER/ORR. CV and LSV measurements were performed at various scan rates (i.e. 10, 25 and 50 mV/s) versus Ag/AgCl for OER and ORR in 0.5 M KOH. Rotating disc electrode experiments were also performed by LSV in O_2-saturated 0.5 M KOH versus Ag/AgCl at various rotation speeds from 500 to 3000 rpm. Koutecky-Levich (K–L) equation was employed to calculate the number of electrons involved in OER/ORR reactions (Wu et al., 2012; Zhou et al., 2016). CA experiments (current density vs time) were conducted at 0.55, 0.65 and 0.75 V in 0.5 M KOH versus Ag/AgCl for stability check.

3. Results and discussion

Phase identification and morphology of the prepared $NiMoO_4$-NRs@RGO nanocomposites were analyzed by XRD and FESEM studies. XRD patterns confirm the presence of $NiMoO_4$ and RGO in the prepared nanocomposite. XRD reflections of $\langle 110\rangle$, $\langle -111\rangle$, $\langle -201\rangle$, $\langle 111\rangle$, $\langle 021\rangle$, $\langle -112\rangle$, $\langle 220\rangle$, $\langle -222\rangle$, $\langle 202\rangle$, $\langle 040\rangle$, $\langle 330\rangle$, $\langle 240\rangle$ and $\langle -204\rangle$ correspond to monoclinic phase of $NiMoO_4$ material (JCPDS#31-0902) while presence of $\langle 002\rangle$ reflection at two theta value of 25.88° belongs to RGO in nanocomposite (Fig. 1a). FESEM study of $NiMoO_4$-NRs@RGO nanocomposites reveals that $NiMoO_4$ nanorods are supported by reduced graphene oxide sheets as expected (Fig. 1b). FTIR spectrum of $NiMoO_4$-NRs@RGO nanocomposites shows two strong bands at ~970 and ~650 cm^{-1} of $NiMoO_4$ (Klissurski et al., 2006; Wan et al., 2013) while FTIR bands at ~1210 and ~1555 cm^{-1} confirm the presence of RGO in the nanocomposites (Fig. 1c). Fig. 1d represents Raman spectrum of $NiMoO_4$-NRs@RGO nanocomposites. The appeared bands at ~704, ~815, ~910 and ~958 cm^{-1} belong to $NiMoO_4$ (Tian et al., 2018) whereas the acted bands at ~1375 and ~1575 cm^{-1} symbolize to RGO (Kumar et al., 2017). BET surface area of $NiMoO_4$-NRs@RGO nanocomposites was found to be ~40 m^2/g from the N_2 adsorption and desorption studies. Fig. 2a shows TEM micrograph of RGO sheets as received. TEM and HER-TEM studies of $NiMoO_4$-NRs@RGO nanocomposites are shown in Fig. 2b and c, respectively. Inset of Fig. 2c shows a clear image of the formation of lattice fringes with d-spacing value of ~3.08 Å correspond to $\langle 220\rangle$ plane of $NiMoO_4$. EDS study of $NiMoO_4$-NRs@RGO nanocomposites also confirms the presence of Ni, Mo and C elements (Fig. 2d). Note that EDS is equipped with TEM machine and the presence of Cu element in EDS is due to Cu based TEM grid.

XPS measurement was carried out for the study of surface composition of the $NiMoO_4$-NRs@RGO nanocomposites as shown in Fig. 3. The appearance of four peaks of C 1s, Mo 3d, O 1s and Ni 2p at ~285, ~233, ~535 and ~856 eV respectively indicate that $NiMoO_4$- NRs are supported by RGO sheets. High resolution XPS spectrum of C 1s is associated with three de-convoluted peaks of C-O, C—C, and C═C (Fig. 3a). High resolution XPS spectrum of Mo 3d shows bands at ~233 and ~238 eV of Mo $3d_{5/2}$ and Mo $3d_{3/2}$, respectively, belong to Mo^{6+} oxidation state (Fig. 3b). Fig. 3c shows high resolution XPS spectrum of O 1s, indicated two de-convoluted peaks at ~532 and ~535 eV for oxygen contributions with metal oxygen bonds and RGO. High resolution XPS spectrum of Ni 2p shows two main bands at ~856 and ~875 eV of Ni $2p_{3/2}$ and Ni $2p_{1/2}$, respectively, with two satellite bands at ~862 and ~880 eV (Fig. 3d). The resulting XPS data is consistent with previous reports (Xu et al., 2018).

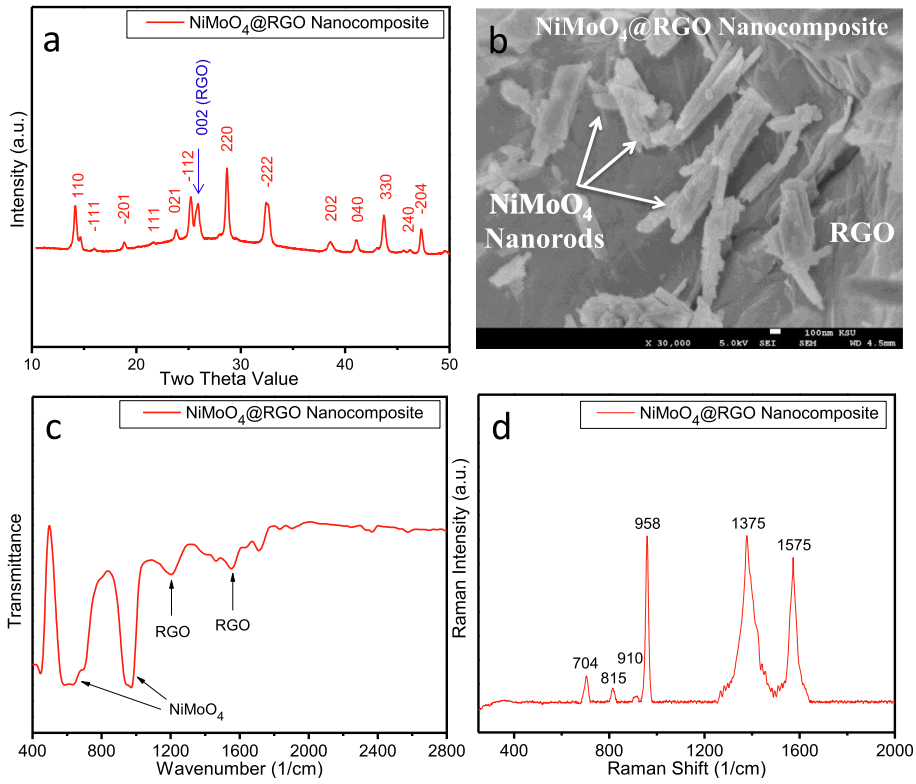

Fig. 1. (a) XRD, (b) FESEM, (c) FTIR, and (d) Raman studies of $NiMoO_4$-NRs@RGO nanocomposites.

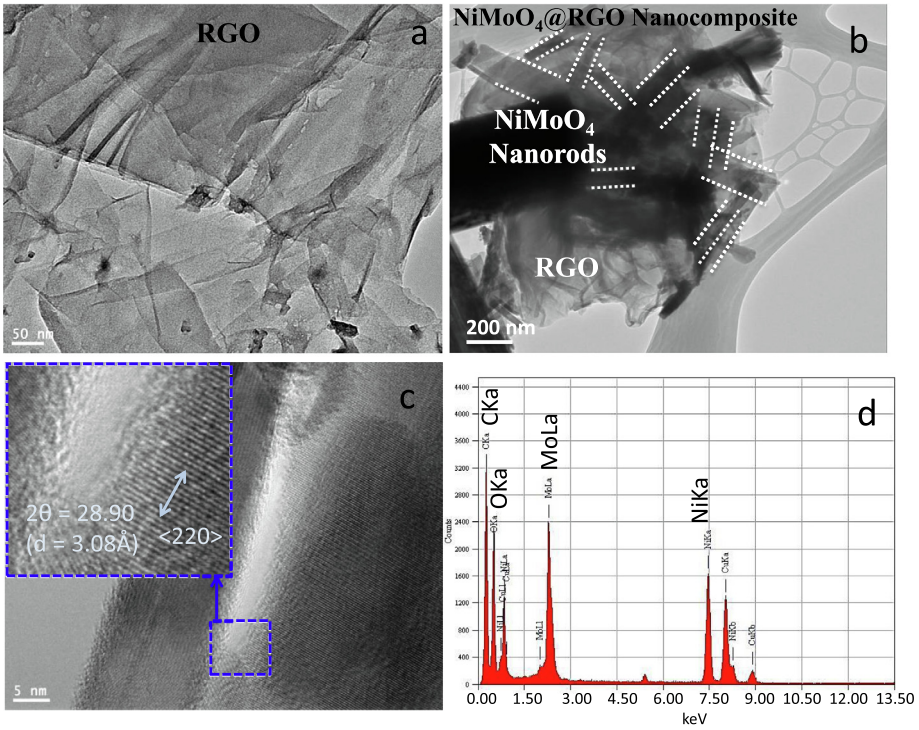

Fig. 2. TEM images of (a) RGO sheets as received, and (b) $NiMoO_4$-NRs@RGO nanocomposites. (c) HRTEM, and (d) EDS studies of $NiMoO_4$-NRs@RGO nanocomposites. Inset of Fig. 2c shows lattice fringes from HRTEM.

The electrochemical properties of $NiMoO_4$-NRs@RGO nanocomposites for bifunctional catalytic activities (OER/ORR) were investigated in 0.5 M KOH. Initially, CV measurements were carried out to check bifunctional electro-catalytic behavior of $NiMoO_4$-NRs@RGO nanocomposites at different scan rates (i.e. 10, 25 and 50 mV/s) under the applied potential range from −1 to +1 V vs Ag/AgCl as shown in Fig. 4a. Thereafter, LSV polarization experiments were conducted to confirm the bifunctional OER and ORR activities of

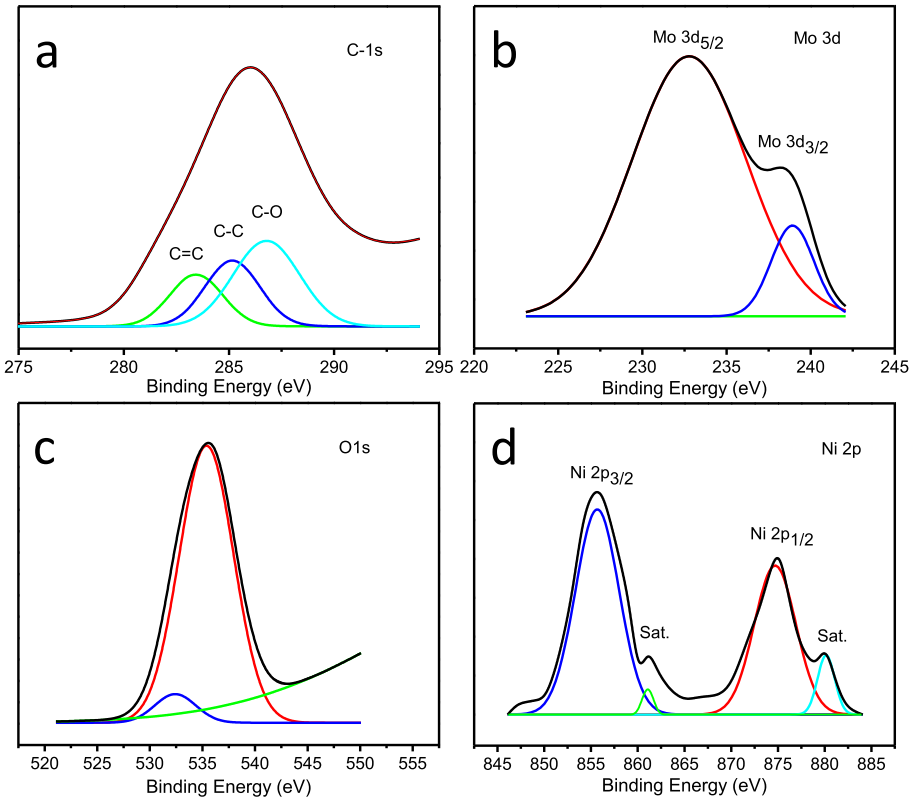

Fig. 3. High resolution XPS spectra of (a) C 1s, (b) Mo 3d, (c) O 1s, and (d) Ni 2p of $NiMoO_4$-NRs@RGO nanocomposites.

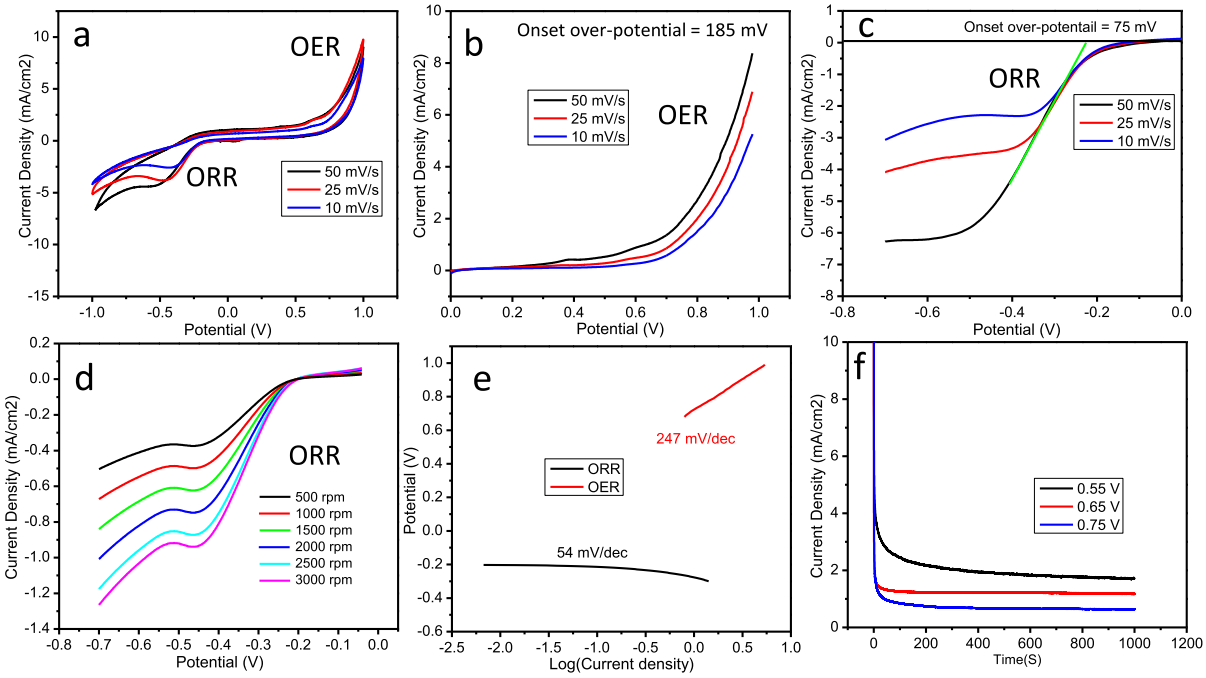

Fig. 4. Electrochemical OER/ORR properties of $NiMoO_4$-NRs@RGO nanocomposites in 0.5 M KOH. (a) CV for OER/ORR. (b) LSV polarization curves for OER. LSV polarization curves (c) at various scan rates, and (d) at various rotations for ORR. (e) Tafel plots for OER/ORR. (f) CA plots for stability of $NiMoO_4$-NRs@RGO nanocomposites.

$NiMoO_4$-NRs@RGO nanocomposites. LSV polarization curves of $NiMoO_4$-NRs@RGO nanocomposite for OER were collected in anodic region under the applied potential window from 0.0 to 1.0 V at the scan rates of 10, 25 and 50 mV/s as displayed in Fig. 4b. We observed that the $NiMoO_4$-NRs@RGO nanocomposites show efficient OER activity with the onset over-potential of ~185 mV, which is even better than that of previously reported OER electro-catalysts. Fig. 4c shows LSV polarization curves of $NiMoO_4$-

NRs@RGO nanocomposites for ORR in cathodic region from 0.0 to −0.7 V at 10, 25 and 50 mV/s. The $NiMoO_4$-NRs@RGO nanocomposites exhibit excellent ORR performance with low onset over-potential of ~75 mV, which is much better than other reported ORR electro-catalysts. LSV polarization studies of $NiMoO_4$-NRs@RGO nanocomposites were also carried out by applying cathodic potential window range using rotating disc electrode at various rotations from 500 to 3000 rpm at 25 mV/s vs Ag/AgCl in O_2-saturated 0.5 M KOH electrolyte for ORR (Fig. 4d). This is noteworthy that the diffusion current densities of $NiMoO_4$-NRs@RGO nanocomposite increase significantly with rotations as expected because of oxygen diffusion distance. The number of electrons involved in water oxidation reactions ($4e^-$) was calculated using the LSV polarization data at various rotations followed by Koutecky–Levich (K–L) equation. Details of K–L equation were also reported elsewhere (Wu et al., 2012; Zhou et al., 2016). The standard reaction for ORR in alkaline medium can be defined as follows: $O_2(g) + 2H_2O(l) + 4e^- \rightarrow 4OH^-$. Tafel plots of $NiMoO_4$-NRs@RGO nanocomposites for OER and ORR at 10 mV/s are shown in Fig. 4e. Tafel studies explain the kinetics of water splitting reactions to OER/ORR depending on the nature and surface area of the materials. Tafel slope values of $NiMoO_4$-NRs@RGO nanocomposites were found to be ~247 and ~54 mV/decade for OER and ORR, respectively, in O_2-saturated 0.5 M KOH vs Ag/AgCl. Note that the experimental error in Tafel slopes to be ±5. Tafel slopes of noble metals oxides (IrO_2, RuO_2) were reported in the range from 45 to 215 mV/decade for OER/ORR (Cruz et al., 2011; Fang and Liu, 2010; Kadakia et al., 2014; Ouattara et al., 2009). Low onset over-potential and low Tafel slopes sustain low energy loss during electro-chemical water splitting reactions. Therefore, based on present results, the $NiMoO_4$-NRs@RGO nanocomposites exhibit excellent electro-catalytic performance in OER/ORR activities. Stability of $NiMoO_4$-NRs@RGO electrode materials was also investigated using potentio-static CA experiments. CA experimentations were conducted at various fixed potentials of 0.55, 0.65 and 0.75 V for 1000 s using the same electrolyte concentration (Fig. 4f). We have observed from CA measurements that the obtained current densities are quite constant at fixed potential with time, which indicates the stable nature of the electrode materials. Moreover, the stability of the $NiMoO_4$-NRs@RGO nanocomposites was also tested from XRD after electro-catalytic measurements as shown in Fig. 5. The sample for XRD was prepared on carbon paper followed by the LSV polarization studies under the similar conditions for OER/ORR. XRD patterns show that the electro-catalyst is quite stable with a small amount of impurity phase detected at two theta of 28.30°. Our results confirmed that $NiMoO_4$-NRs@RGO nanocomposites are quite stable and could be used as an alternate of noble metal oxides electro-catalysts for energy conversion as future electro-catalysts.

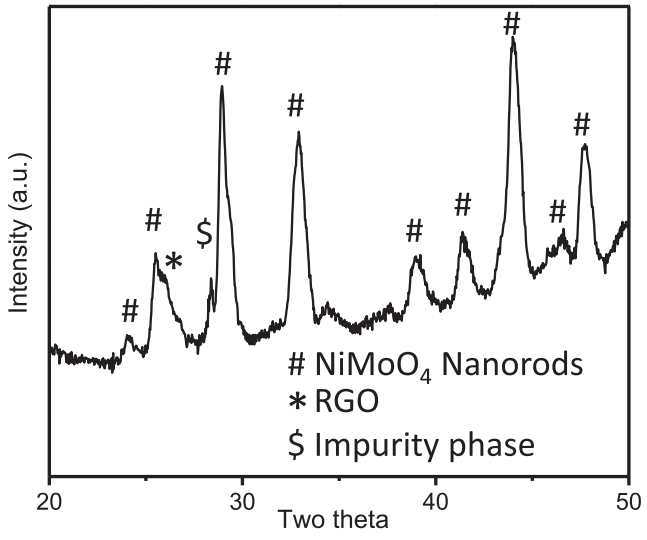

Fig. 5. XRD patterns of $NiMoO_4$-NRs@RGO nanocomposites after electro-catalysis.

4. Conclusions

We conclude present work that $NiMoO_4$-NRs@RGO nanocomposites were synthesized by hydrothermal process. The prepared $NiMoO_4$-NRs@RGO nanocomposites show excellent electrochemical performance in alkaline medium (0.5 M KOH). The $NiMoO_4$-NRs@RGO nanocomposites exhibit low onset over-potentials (~75 mV for ORR, ~185 mV for OER) and low Tafel slopes (~247 mV/dec for ORR and ~54 mV/dec for OER) with $4e^-$ system in redox reactions. Therefore, low cost $NiMoO_4$-NRs@RGO nanocomposites show admirable electro-catalytic performance with low energy loss and could be an alternate of expensive electro-catalysts.

Declaration of Competing Interest

The authors declare that they have no known competing financial interests or personal relationships that could have appeared to influence the work reported in this paper.

Acknowledgement

The authors extend their grateful appreciation to the Deanship of Scientific Research at King Saud University for funding their research group (RG-1439-087).

References

Abbas, Y., Yun, S., Javed, M.S., Chen, J., Tahir, M.F., Wang, Z., Yang, C., Arshad, A., Hussain, S., 2020. Anchoring 2D NiMoO4 nano-plates on flexible carbon cloth as a binder-free electrode for efficient energy storage devices. Ceram. Int. 46 (4), 4470–4476. https://doi.org/10.1016/j.ceramint.2019.10.173.

Ahmed, J., Ahamad, T., Alhokbany, N., Almaswari, B.M., Ahmad, T., Hussain, A., Al-Farraj, E.S.S., Alshehri, S.M., 2018. Molten salts derived copper tungstate nanoparticles as bifunctional electro-catalysts for electrolysis of water and supercapacitor applications. ChemElectroChem 5 (24), 3938–3945. https://doi.org/10.1002/celc.201801196.

Ahmed, J., Mao, Y., 2016. Ultrafine iridium oxide nanorods synthesized by molten salt method toward electrocatalytic oxygen and hydrogen evolution reactions. Electrochim. Acta 212, 686–693. https://doi.org/10.1016/j.electacta.2016.06.122.

Ahmed, J., Ubaidullah, M., Ahmad, T., Alhokbany, N., Alshehri, S.M., 2019a. Synthesis of graphite oxide/cobalt molybdenum oxide hybrid nanosheets for enhanced electrochemical performance in supercapacitors and the oxygen evolution reaction. ChemElectroChem 6 (9), 2524–2530. https://doi.org/10.1002/celc.201900055.

Ahmed, J., Ubiadullah, M., Alhokbany, N., Alshehri, S.M., 2019b. Synthesis of ultrafine NiMoO4 nano-rods for excellent electro-catalytic performance in hydrogen evolution reactions 126696 Mater. Lett. 257. https://doi.org/10.1016/j.matlet.2019.126696.

Alshehri, S.M., Ahmed, J., Ahamad, T., Alhokbany, N., Arunachalam, P., Al-Mayouf, A. M., Ahmad, T., 2018. Synthesis, characterization, multifunctional electrochemical (OGR/ORR/SCs) and photodegradable activities of ZnWO4 nanobricks. J. Sol-Gel Sci. Technol. 87 (1), 137–146. https://doi.org/10.1007/s10971-018-4698-7.

AlShehri, S., Ahmed, J., Ahamad, T., Arunachalam, P., Ahmad, T., Khan, A., 2017. Bifunctional electro-catalytic performances of CoWO 4 nanocubes for water redox reactions (OER/ORR). RSC Adv. 7 (72), 45615–45623. https://doi.org/10.1039/C7RA07256B.

An, L., Zang, X., Ma, L., Guo, J., Liu, Q., Zhang, X., 2020. Graphene layer encapsulated MoNi4-NiMoO4 for electrocatalytic water splitting. Appl. Surf. Sci. 504. https://doi.org/10.1016/j.apsusc.2019.144390. 144390.

Anil Kumar, Y., Singh, S., Kulurumotlakatla, D.K., Kim, H.-J., 2020. A MoNiO4 flower-like electrode material for enhanced electrochemical properties via a facile chemical bath deposition method for supercapacitor applications. New J. Chem. 44 (2), 522–529. https://doi.org/10.1039/C9NJ05529K.

Cai, D., Liu, B., Wang, D., Liu, Y., Wang, L., Li, H., Wang, Y., Wang, C., Li, Q., Wang, T., 2014. Enhanced performance of supercapacitors with ultrathin mesoporous NiMoO4 nanosheets. Electrochim. Acta 125, 294–301. https://doi.org/10.1016/j.electacta.2014.01.049.

Cruz, J.C., Baglio, V., Siracusano, S., Ornelas, R., Ortiz-Frade, L., Arriaga, L.G., Antonucci, V., Aricò, A.S., 2011. Nanosized IrO2 electrocatalysts for oxygen evolution reaction in an SPE electrolyzer. J. Nanopart. Res. 13 (4), 1639–1646. https://doi.org/10.1007/s11051-010-9917-2.

Fang, D., Zhang, H., He, L., Geng, J., Song, W., Sun, S., Shao, Z., Yi, B., 2019. Facile synthesis of nanoporous Pt-encapsulated Ir black as a bifunctional oxygen catalyst via modified polyol process at room temperature. ChemElectroChem 6 (14), 3633–3643. https://doi.org/10.1002/celc.201900824.

Fang, Y.-H., Liu, Z.-P., 2010. Mechanism and Tafel lines of electro-oxidation of water to oxygen on RuO2(110). J. Am. Chem. Soc. 132 (51), 18214–18222. https://doi.org/10.1021/ja1069272.

Feng, X., Ning, J., Wang, D., Zhang, J., Xia, M., Wang, Y., Hao, Y., 2020. Heterostructure arrays of NiMoO4 nanoflakes on N-doping of graphene for high-performance asymmetric supercapacitors. J. Alloy. Compd. 816. https://doi.org/10.1016/j.jallcom.2019.152625. 152625.

Geng, S., Yang, W., Yu, Y., 2019. Fabrication of NiC/MoC/NiMoO4 heterostructured nanorod arrays as stable bifunctional electrocatalysts for efficient overall water splitting. Chem. Asian J. 14 (7), 1013–1020. https://doi.org/10.1002/asia.201801871.

Jiang, G., Li, L.i., Xie, Z., Cao, B., 2019. Facile fabrication of porous NiMoO4@C nanowire as high performance anode material for lithium ion batteries. Ceram. Int. 45 (15), 18462–18470. https://doi.org/10.1016/j.ceramint.2019.06.064.

Jinlong, L.v., Miura, H., Meng, Y., 2017. A novel mesoporous NiMoO4@rGO nanostructure for supercapacitor applications. Mater. Lett. 194, 94–97. https://doi.org/10.1016/j.matlet.2017.02.040.

Kadakia, K., Datta, M.K., Velikokhatnyi, O.I., Jampani, P.H., Kumta, P.N., 2014. Fluorine doped (Ir,Sn,Nb)O2 anode electro-catalyst for oxygen evolution via PEM based water electrolysis. Int. J. Hydrogen Energy 39 (2), 664–674. https://doi.org/10.1016/j.ijhydene.2013.10.123.

Karami, C., Taher, M.A., 2019. A novel enzyme-less amperometric sensor for hydrogen peroxide based on nickel molybdate nanoparticles. J. Electroanal. Chem. 847, 113219. https://doi.org/10.1016/j.jelechem.2019.113219.

Kasturi, P.R., Shanmugapriya, S., Elizabeth, M., Athira, K., Selvan, R.K., 2020. Electrocatalytic hydrogen evolution reaction studies of NiW1−xMoxO4 (x = 0.0, 0.5 and 1.0) nanoparticles in both acid and alkaline electrolytes. J. Mater. Sci.: Mater. Electron. 31 (3), 2378–2387. https://doi.org/10.1007/s10854-019-02773-0.

Klissurski, D., Mancheva, M., Iordanova, R., Tyuliev, G., Kunev, B., 2006. Mechanochemical synthesis of nanocrystalline nickel molybdates. J. Alloys Compd. 422 (1-2), 53–57. https://doi.org/10.1016/j.jallcom.2005.11.073.

Kumar, R., Gupta, P.K., Agrawal, A., Nagarale, R.K., Sharma, A., 2017. Hydrothermally synthesized reduced graphene oxide-NiWO4 nanocomposite for lithium-ion battery anode. J. Electrochem. Soc. 164 (4), A785–A795. https://doi.org/10.1149/2.1181704jes.

Lu, X., Cai, M., Huang, J., Xu, C., 2020. Ultrathin and porous Mo-doped Ni nanosheet arrays as high-efficient electrocatalysts for hydrogen evolution reaction. J. Colloid Interface Sci. 562, 307–312. https://doi.org/10.1016/j.jcis.2019.12.001.

Moosavifard, S.E., Shamsi, J., Ayazpour, M., 2015. 2D high-ordered nanoporous NiMoO4 for high-performance supercapacitors. Ceram. Int. 41 (1), 1831–1837. https://doi.org/10.1016/j.ceramint.2014.09.130.

Ouattara, L., Fierro, S., Frey, O., Koudelka, M., Comninellis, C., 2009. Electrochemical comparison of IrO2 prepared by anodic oxidation of pure iridium and IrO2 prepared by thermal decomposition of H2IrCl6 precursor solution. J. Appl. Electrochem. 39 (8), 1361–1367. https://doi.org/10.1007/s10800-009-9809-2.

Oudghiri-Hassani, H., Al Wadaani, F., 2018. Preparation, characterization and catalytic activity of nickel molybdate (NiMoO4) nanoparticles. Molecules 23, 273.

Ray, S.K., Dhakal, D., Lee, S.W., 2018. Insight into malachite green degradation, mechanism and pathways by morphology-tuned α-nimoo4 photocatalyst. Photochem. Photobiol. 94, 552–563. https://doi.org/10.1111/php.12872.

Reier, T., Oezaslan, M., Strasser, P., 2012. Electrocatalytic oxygen evolution reaction (OER) on Ru, Ir, and Pt catalysts: a comparative study of nanoparticles and bulk materials. ACS Catal. 2 (8), 1765–1772. https://doi.org/10.1021/cs3003098.

Shaner, M.R., Atwater, H.A., Lewis, N.S., McFarland, E.W., 2016. A comparative technoeconomic analysis of renewable hydrogen production using solar energy. Energy Environ. Sci. 9 (7), 2354–2371. https://doi.org/10.1039/C5EE02573G.

Tian, X., Li, X., Yang, T., Wang, K., Wang, H., Song, Y., Liu, Z., Guo, Q., 2018. Porous worm-like NiMoO4 coaxially decorated electrospun carbon nanofiber as binder-free electrodes for high performance supercapacitors and lithium-ion batteries. Appl. Surf. Sci. 434, 49–56. https://doi.org/10.1016/j.apsusc.2017.09.153.

Tong, B., Wei, W., Chen, X., Wang, J., Ye, W., Cui, S., Chen, W., Mi, L., 2019. Designed synthesis of porous NiMoO 4/C composite nanorods for asymmetric supercapacitors. CrystEngComm 21 (36), 5492–5499. https://doi.org/10.1039/C9CE01031A.

Wan, H., Jiang, J., Ji, X., Miao, L., Zhang, L.i., Xu, K., Chen, H., Ruan, Y., 2013. Rapid microwave-assisted synthesis NiMoO4·H2O nanoclusters for supercapacitors. Mater. Lett. 108, 164–167. https://doi.org/10.1016/j.matlet.2013.06.099.

Wang, J., Li, L., Meng, L., Wang, L., Liu, Y., Li, W., Sun, W., Li, G., 2018. Morphology engineering of nickel molybdate hydrate nanoarray for electrocatalytic overall water splitting: from nanorod to nanosheet. RSC Adv. 8 (61), 35131–35138. https://doi.org/10.1039/C8RA07323F.

Wang, Y.-Q., Zhao, L., Sui, X.-L., Gu, D.-M., Wang, Z.-B., 2019. Hierarchical CoP3/NiMoO4 heterostructures on Ni foam as an efficient bifunctional electrocatalyst for overall water splitting. Ceram. Int. 45 (14), 17128–17136. https://doi.org/10.1016/j.ceramint.2019.05.266.

Wu, Z., Li, W., Xia, Y., Webley, P., Zhao, D., 2012. Ordered mesoporous graphitized pyrolytic carbon materials: synthesis, graphitization, and electrochemical properties. J. Mater. Chem. 22 (18), 8835. https://doi.org/10.1039/c2jm30192j.

Xu, Y., Xuan, H., Gao, J., Liang, T., Han, X., Yang, J., Zhang, Y., Li, H., Han, P., Du, Y., 2018. Hierarchical three-dimensional NiMoO4-anchored rGO/Ni foam as advanced electrode material with improved supercapacitor performance. J. Mater. Sci. 53 (11), 8483–8498. https://doi.org/10.1007/s10853-018-2171-1.

Yang, D., Yang, L., Zhong, L., Yu, X.u., Feng, L., 2019. Urea electro-oxidation efficiently catalyzed by nickel-molybdenum oxide nanorods. Electrochim. Acta 295, 524–531. https://doi.org/10.1016/j.electacta.2018.10.190.

Zhang, S., She, G., Li, S., Qu, F., Mu, L., Shi, W., 2019. Enhancing the electrocatalytic activity of NiMoO4 through a post-phosphorization process for oxygen evolution reaction. Catal. Commun. 129, 105725. https://doi.org/10.1016/j.catcom.2019.105725.

Zhang, Z., Ma, X., Tang, J., 2018. Porous NiMoO 4−x/MoO2 hybrids as highly effective electrocatalysts for the water splitting reaction. J. Mater. Chem. A 6 (26), 12361–12369. https://doi.org/10.1039/C8TA03047B.

Zhou, R., Zheng, Y., Jaroniec, M., Qiao, S.-Z., 2016. Determination of the electron transfer number for the oxygen reduction reaction: from theory to experiment. ACS Catal. 6 (7), 4720–4728. https://doi.org/10.1021/acscatal.6b01581.s001.